Supplementary Data for Manuscript Entitled
Preclinical development of a Molecular Clamp Stabilised Subunit Vaccine for SARS-CoV-2

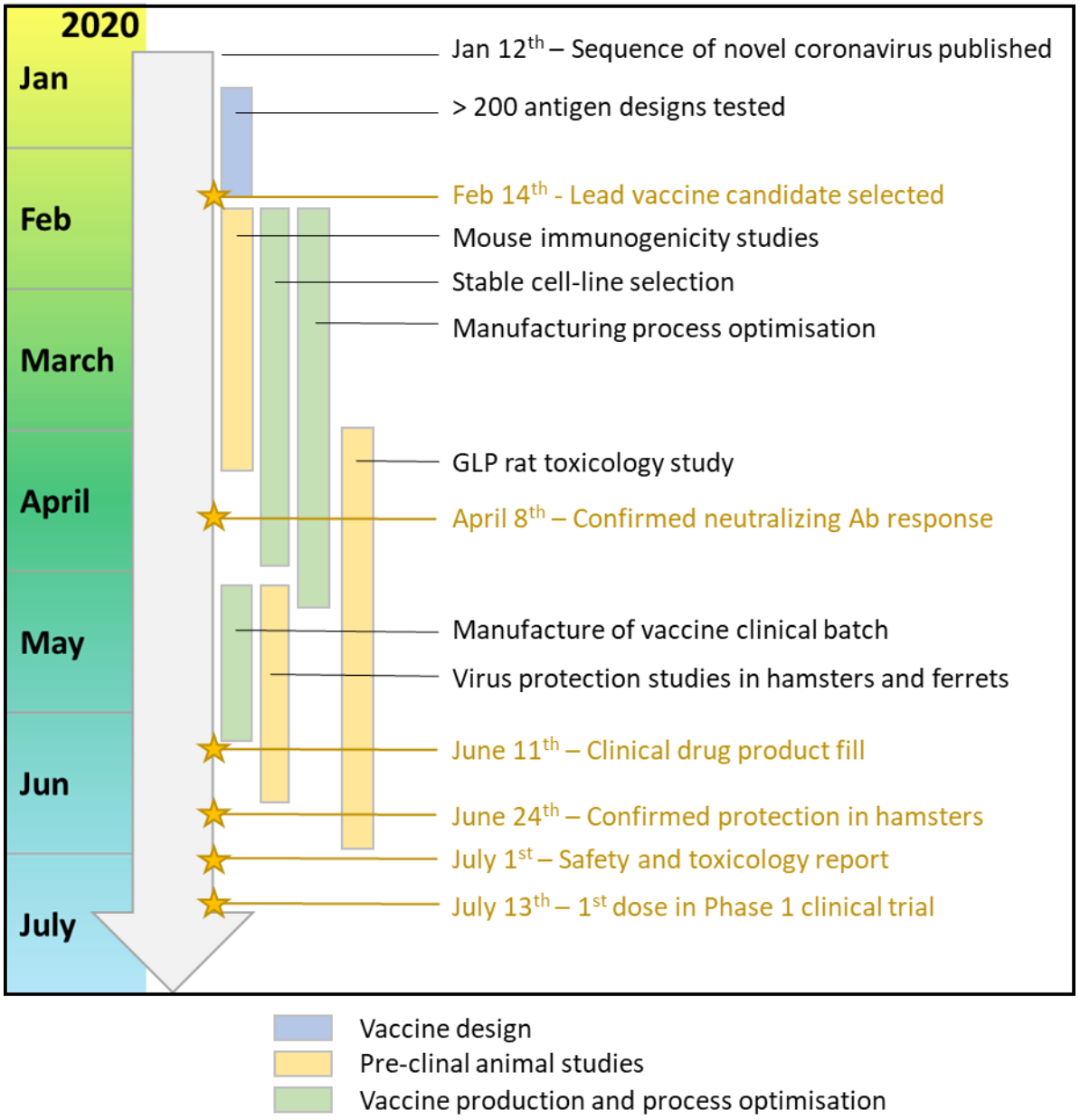

Supplementary figure 1. Timeline summarising the preclinical development of the SARS-CoV-2 Sclamp vaccine.

Supplementary Data for Manuscript Entitled

Preclinical development of a Molecular Clamp Stabilised Subunit Vaccine for SARS-CoV-2

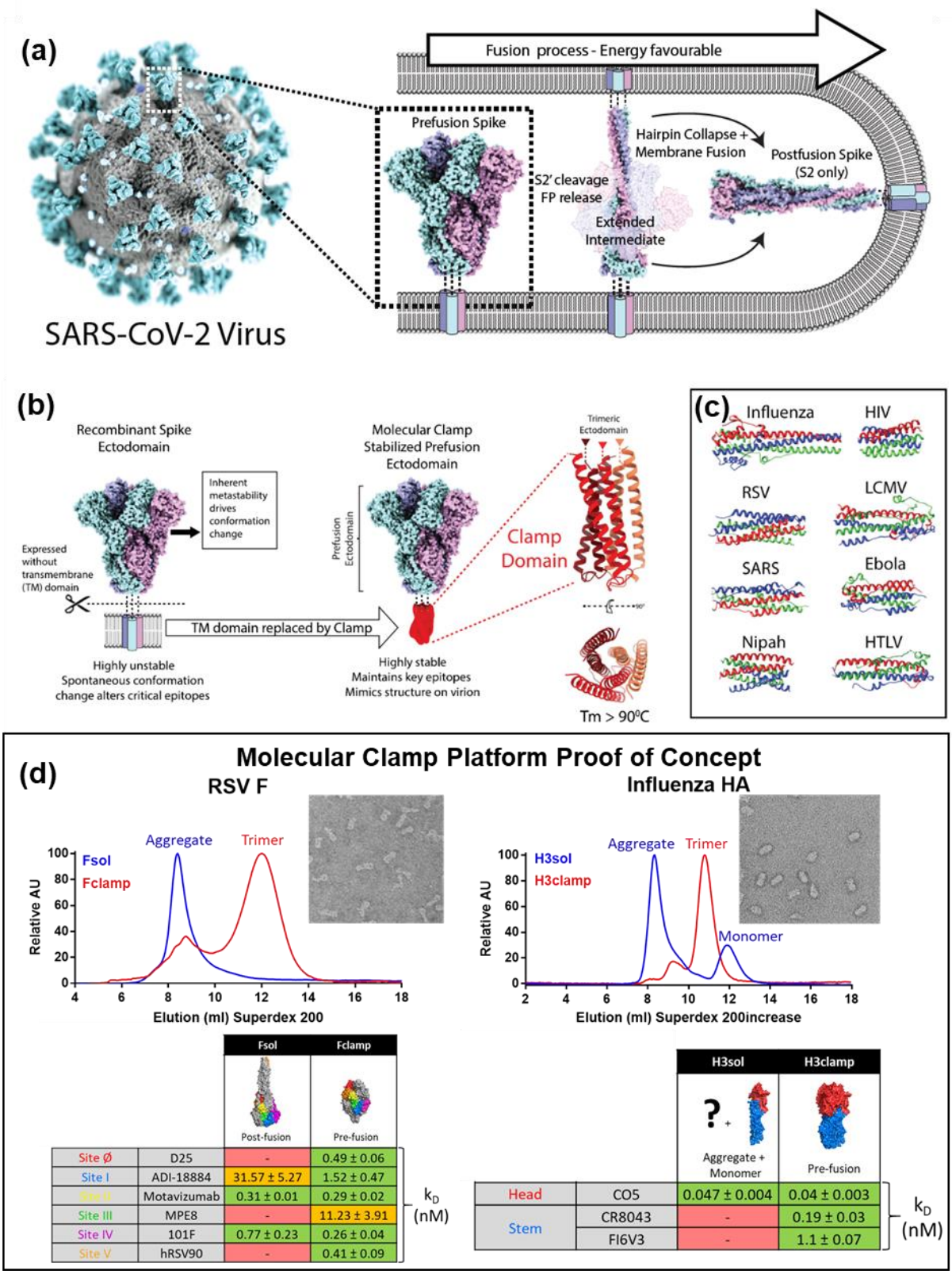

Supplementary figure 2. Overview of the molecular clamp platform. **(a)** Schematic representing the SARS-CoV-2 virion, spike protein and the transition process from the pre-fusion conformation to the post-fusion conformation. **(b)** Schematic representation of how the molecular clamp six helical bundle is inserted in place of the spike protein transmembrane domain to produce a soluble protein that is stabilized in the pre-fusion conformation. **(c)** Representative image showing the conserved architecture of the six-

helical bundles from viral fusion protein that can be used as molecular clamps to achieve pre-fusion stabilization. RSV – respiratory syncytial virus (RSV); LCMV – lymphocytic choriomeningitis virus; HTLV – human T-cell leukemia virus type 1. **(d)** Proof of concept examples for the molecular clamp platform technology. Addition of the molecular clamp to the ectodomain of RSV Fusion (F) and Influenza A Haemagglutinin (HA) proteins facilitates the purification of soluble trimeric protein as assessed by size-exclusion chromatography and negative stain transmission electron microscopy. The clamp stabilised antigens are recognised by pre-fusion specific antibodies D25,[1] MPE8,[2] hRSV90,[3] CR8043,[4] and FI6V3.[5]

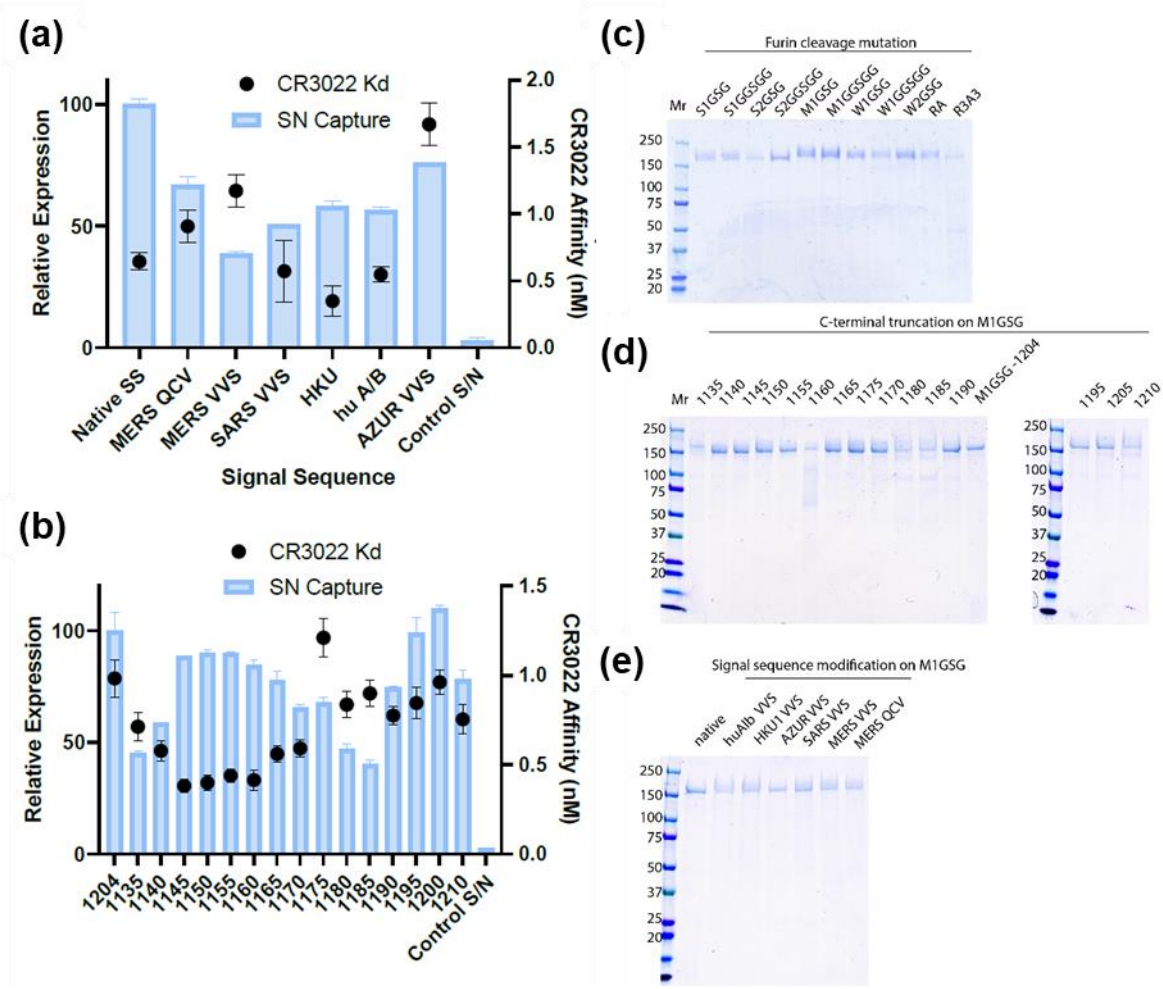

Supplementary figure 3. SDS-PAGE analysis of Sclamp vaccine candidates. **(a)** In vitro screening of signal peptide sequence for yield and CR3022 affinity (K_D). **(b)** In vitro screening of C-terminal length changes for yield and CR3022 affinity (K_D). **(c)** Furin cleavage mutation constructs, **(d)** C-terminal truncation on M1GSG backbone, **(e)** Signal sequence modification on M1GSG backbone. Two micrograms of proteins were prepared in reduced condition, boiled and loaded onto 4-15% SDS-PAGE gel. The proteins were visualized by Coomassie staining.

Supplementary Data for Manuscript Entitled

Preclinical development of a Molecular Clamp Stabilised Subunit Vaccine for SARS-CoV-2

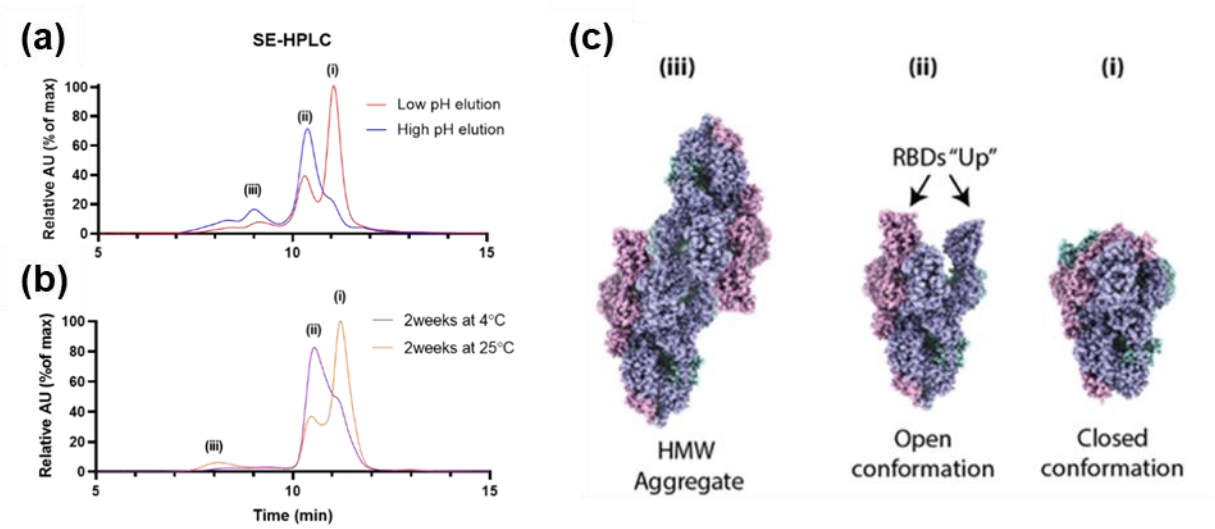

Supplementary figure 4. Separation of SARS-Cov-2 Sclamp conformations by analytical SE-HPLC. **(a)** Analytical SE-HPLC separation of low and high pH eluted SARS-CoV-2 Sclamp showing the presence of three peaks designate i, ii, and iii. For the purification, supernatant from the Sclamp encoding DNA (M1 GSG) was added to anti-clamp protein affinity column that was pre-equilibrated with high salt PBS (PBS with 400 mM NaCl, pH 7.4). Bound resin was washed with 15 column volumes (CV) of high salt PBS before elution with either high pH buffer (100 mM glycine, 137 mM NaCl, 5 mM EDTA, pH 11.5) or low pH buffer (100 mM Sodium Acetate, 100 mM NaCl, pH 3.5). **(b)** Analytical SE-HPLC separation of SARS-CoV-2 Sclamp following 2-week incubation at 4ºC or 25ºC showing the presence of three peaks designated i, ii, and iii. **(c)** Hypothesis describing the structure of SARS-CoV-2 Sclamp present at each peak present on the HPLC trace and how the antigen may transition between the two previously described Spike conformations, termed 'open' and 'closed', and a high molecular weight (HMV) aggregated product.

Supplementary Data for Manuscript Entitled
Preclinical development of a Molecular Clamp Stabilised Subunit Vaccine for SARS-CoV-2

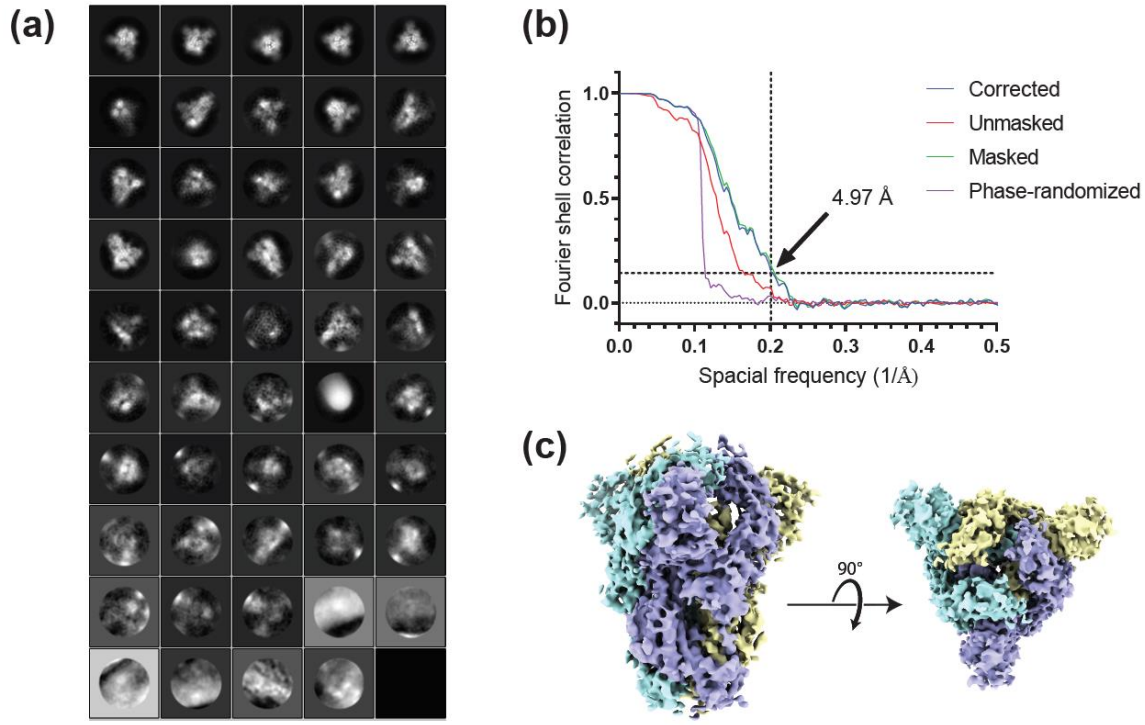

Supplementary figure 5. Cryo-EM single particle analysis of Sclamp. Purified SARS-CoV-2 Sclamp was plunge frozen on TEM grids and imaged by cryo-EM. Data was acquired on a CryoARM-300 equipped with a K3 camera. **(a)** 2D class averages of the Sclamp particles with an imposed spherical mask of 250 Å were generated by RELION 3.1. **(b)** Fourier shell correlation analysis of single particle analysis 3D refinement with C3 symmetry, indicating a final resolution of 4.97 Å at a Fourier shell correlation cut-off of 0.143. **(c)** Side-on and top down representations of the Sclamp cryo-EM map with the 3 S protein monomers coloured individually for clarity.

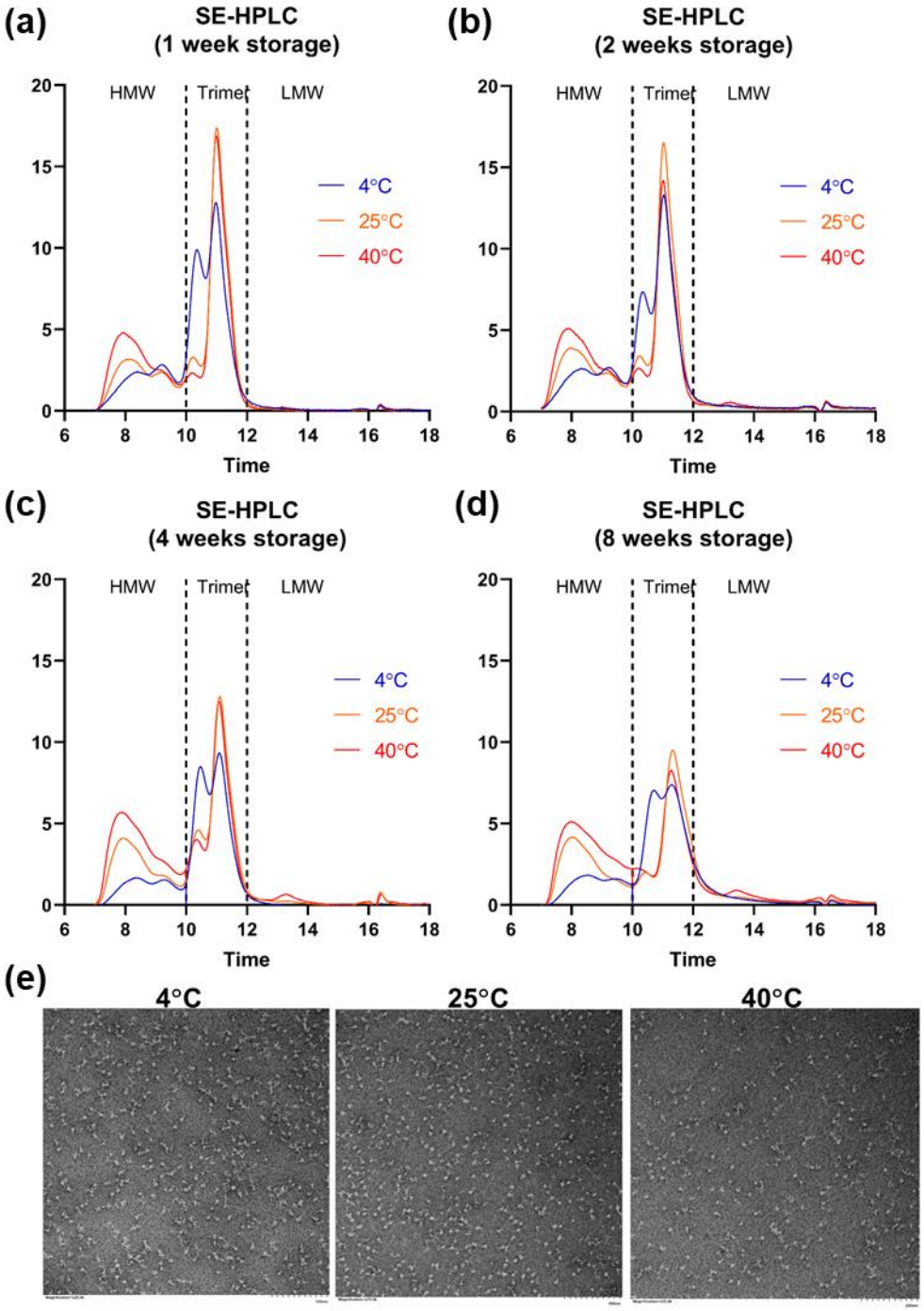

Supplementary figure 6. Thermal stability and separation of SARS-CoV-2 Sclamp conformations by analytical SE-HPLC. **(a-d)** Purified SARS-CoV-2 Sclamp was incubated for either 1 (a), 2 (b), 4 (c) or 8 (d) weeks at 4°C, 25°C or 40°C before separation by SE-HPLC. **(e)** Negative stain images of SARS-CoV Sclamp stored for 4 weeks at 4°C, 25°C or 40°C, and imaged using a Hitachi HT7700 microscope operated at 120 kV, at the magnification of 25,000X using high contrast mode. Pre-fusion conformation of Sclamp was observed across the different thermal stress conditions.

Supplementary Data for Manuscript Entitled

Preclinical development of a Molecular Clamp Stabilised Subunit Vaccine for SARS-CoV-2

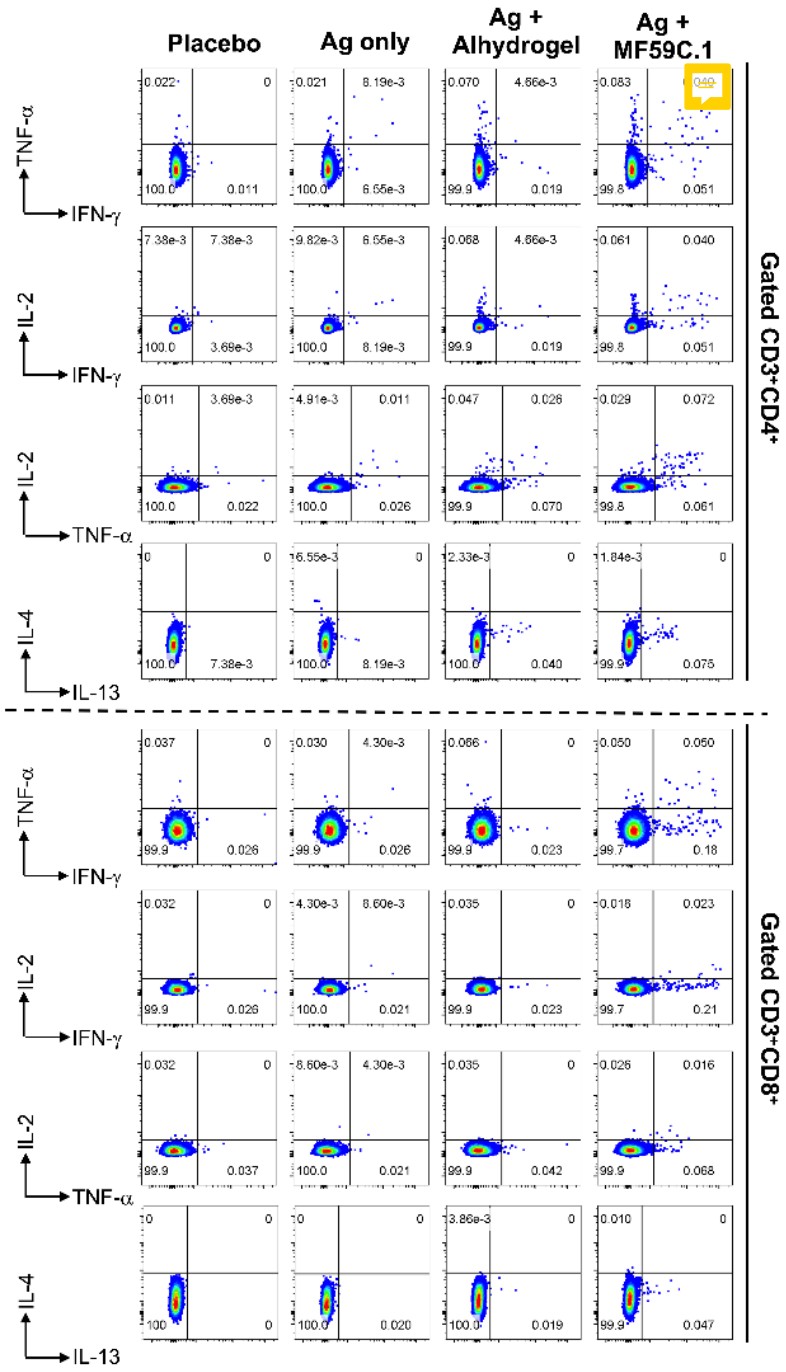

Supplementary figure 7. Representative plots showing the expression of IFN-γ, TNF-α, IL-2, IL-4 and/or IL-13 on gated $CD3^+CD4^+$ (top panel) or $CD3^+CD8^+$ (bottom panel) cells in placebo or SARS-CoV-2 Sclamp vaccinated mice analysed in Figure 3d.

Supplementary Data for Manuscript Entitled

Preclinical development of a Molecular Clamp Stabilised Subunit Vaccine for SARS-CoV-2

Supplementary table 1. Engineered Sclamp variants

Construct	Linker sequence	C-terminus (aa)
Cycle 1		
Wildtype (R/S - furin site)	671 CASYQTQTNSPRRARSVASQSIIAY 695	1204
S1_GSG	671 CASYQGSG----------SIIAY 695	1204
S1GGSGG	671 CASYQGGSGG----------SIIAY 695	1204
S2GSG	671 CASYQTQGSG----------SQSIIAY 695	1204
S2GGSGG	671 CASYQTQGGSGG----------SQSIIAY 695	1204
M1GSG	671 CASYQTQTNGSG----------SIIAY 695	1204
M1GGSGG	671 CASYQTQTNGGSGG---------- SIIAY 695	1204
W1GSG	671 CASYQTQTNSPGSG-SVASQSIIAY 695	1204
W1GGSG	671 CASYQTQTNSPGGSGSVASQSIIAY 695	1204
W2GSG	671 CASYQTQTGSG---------VASQSIIAY 695	1204
W2GGSGG	671 CASYQTQTGGSGG-----VASQSIIAY 695	1204
RA KO	671 CASYQTQTNSPRRAASVASQSIIAY 695	1204
AAAA KO	671 CASYQTQTNSPAAAASVASQSIIAY 695	1204

C-terminal truncation		
	Linker sequence	C-terminus (aa)
M1GSG	671 CASYQTQTNGSGSIIAY 695	1135
		1140
		1145
		1150
		1155
		1160
		1165
		1170
		1175
		1180
		1185
		1190
		1195
		1200
		1205
		1210

Signal sequence modification			C-terminus (aa)
	Sequence		
SARS-CoV2 SS	MFVFLVLLPLVSSQCV	671 CASYQTQTNGSGSIIAY 695	1204
MERS SS VSS	MIHSVFLLMFLLTPTESVSSQCV		1204
MERS SS QCV	MIHSVFLLMFLLTPTESQCV		1204
SARS-CoV1 SS	MFIFLLFLTLTSGVSSQCV		1204
HKU SS	MFLIIFILPTTLAVSSQCV		1204
Azur SS	MTRLTVLALLAGLLASSRAVSSQCV		1204
Hu A/b	MKWVTFISLLFLFSSAYSVSSQCV		1204

Supplementary table 2. P values for the GMFI of CD69 data in Figure 3c

Peptide pool	Groups[Ω] compared	[Ψ]*P*-value	Peptide pool	Comparison	*P*-value
P1	1 vs 2	ns	P7	1 vs 2	ns
	1 vs 3	ns		1 vs 3	ns
	1 vs 4	ns		1 vs 4	0.009
	2 vs 3	ns		2 vs 3	ns
	2 vs 4	ns		2 vs 4	0.009
	3 vs 4	ns		3 vs 4	0.009
P2	1 vs 2	ns	S1	1 vs 2	0.009
	1 vs 3	ns		1 vs 3	0.009
	1 vs 4	0.009		1 vs 4	0.009
	2 vs 3	ns		2 vs 3	0.028
	2 vs 4	0.009		2 vs 4	0.009
	3 vs 4	0.028		3 vs 4	0.009
P3	1 vs 2	0.047	S2	1 vs 2	0.009
	1 vs 3	0.009		1 vs 3	0.009
	1 vs 4	0.009		1 vs 4	0.009
	2 vs 3	ns		2 vs 3	0.016
	2 vs 4	0.009		2 vs 4	0.009
	3 vs 4	0.009		3 vs 4	0.016
P4	1 vs 2	ns	Total	1 vs 2	0.016
	1 vs 3	0.009		1 vs 3	0.009
	1 vs 4	0.009		1 vs 4	0.009
	2 vs 3	0.016		2 vs 3	0.028
	2 vs 4	0.009		2 vs 4	0.009
	3 vs 4	0.009		3 vs 4	0.028
P5	1 vs 2	0.028	Peptivator	1 vs 2	ns
	1 vs 3	0.009		1 vs 3	0.009
	1 vs 4	0.009		1 vs 4	0.009
	2 vs 3	0.016		2 vs 3	0.009
	2 vs 4	0.009		2 vs 4	0.009
	3 vs 4	0.009		3 vs 4	0.028
P6	1 vs 2	ns			
	1 vs 3	0.009			
	1 vs 4	0.009			
	2 vs 3	0.009			
	2 vs 4	0.009			
	3 vs 4	0.028			

[Ω]Groups: 1 = Placebo, 2 = Ag only, 3 = Ag + Alhydrogel and 4 = Ag + MF59C.1

[Ψ]For homoscedastic data sets exhibiting a normal distribution, one-way ANOVA with Tukey's multiple comparison *post-hoc* test was used to calculate the p values. For all heteroscedastic data sets, Welch's ANOVA with Games-Howell *post-hoc* analysis was used to calculate the p values. The *P*-values for non-normally distributed and homoscedastic data sets were calculated using a Kruskal-Wallis *H*-test.

Supplementary Data for Manuscript Entitled

Preclinical development of a Molecular Clamp Stabilised Subunit Vaccine for SARS-CoV-2

Supplementary table 3. *P*-values for the % killed data in Figure 3c

Peptide pool	$^{\Omega}$Groups compared	$^{\Psi}$*P*-value	Peptide pool	Comparison	*P*-value
P1	1 vs 2	ns	P7	1 vs 2	ns
	1 vs 3	ns		1 vs 3	ns
	1 vs 4	ns		1 vs 4	ns
	2 vs 3	ns		2 vs 3	ns
	2 vs 4	ns		2 vs 4	0.027
	3 vs 4	ns		3 vs 4	ns
P2	1 vs 2	ns	S1	1 vs 2	0.028
	1 vs 3	ns		1 vs 3	0.009
	1 vs 4	0.009		1 vs 4	0.009
	2 vs 3	ns		2 vs 3	ns
	2 vs 4	0.009		2 vs 4	0.009
	3 vs 4	0.009		3 vs 4	0.009
P3	1 vs 2	ns	S2	1 vs 2	ns
	1 vs 3	ns		1 vs 3	ns
	1 vs 4	0.001		1 vs 4	<0.0001
	2 vs 3	ns		2 vs 3	0.046
	2 vs 4	0.002		2 vs 4	<0.0001
	3 vs 4	0.013		3 vs 4	0.028
P4	1 vs 2	ns	Total	1 vs 2	0.047
	1 vs 3	0.028		1 vs 3	0.009
	1 vs 4	0.009		1 vs 4	0.009
	2 vs 3	ns		2 vs 3	ns
	2 vs 4	0.009		2 vs 4	0.009
	3 vs 4	0.009		3 vs 4	0.009
P5	1 vs 2	ns	Peptivator	1 vs 2	ns
	1 vs 3	ns		1 vs 3	0.010
	1 vs 4	0.003		1 vs 4	<0.0001
	2 vs 3	ns		2 vs 3	ns
	2 vs 4	0.001		2 vs 4	<0.0001
	3 vs 4	ns		3 vs 4	0.013
P6	1 vs 2	ns			
	1 vs 3	ns			
	1 vs 4	ns			
	2 vs 3	ns			
	2 vs 4	ns			
	3 vs 4	ns			

$^{\Omega}$Groups: 1 = Placebo, 2 = Ag only, 3 = Ag + Alhydrogel and 4 = Ag + MF59C.1

$^{\Psi}$*P*-values were calculated as described in Supplementary table 2.

Supplementary table 4. *P*-values for the $CD3^+CD4^+$ T cell data in Figure 3d

Population	Groups$^{\Omega}$ compared	$^{\Psi}$*P*-value	Population	Groups compared	*P*-value
IFN-γ^+ TNF-α^- IL-2^-	1 vs 2	ns	IFN-γ^- TNF-α^+ IL-2^+	1 vs 2	0.002
	1 vs 3	ns		1 vs 3	<0.0001
	1 vs 4	0.009		1 vs 4	<0.0001
	2 vs 3	ns		2 vs 3	ns
	2 vs 4	0.009		2 vs 4	<0.001
	3 vs 4	0.009		3 vs 4	0.004
IFN-γ^- TNF-α^+ IL-2^-	1 vs 2	ns	IFN-γ^+ TNF-α^+ IL-2^+	1 vs 2	ns
	1 vs 3	ns		1 vs 3	ns
	1 vs 4	0.008		1 vs 4	0.008
	2 vs 3	ns		2 vs 3	ns
	2 vs 4	0.009		2 vs 4	0.009
	3 vs 4	ns		3 vs 4	0.009
IFN-γ^- TNF-α^- IL-2^+	1 vs 2	ns	IFN-γ^- IL-4^+ IL-13^-	1 vs 2	ns
	1 vs 3	0.028		1 vs 3	ns
	1 vs 4	0.009		1 vs 4	ns
	2 vs 3	ns		2 vs 3	ns
	2 vs 4	0.009		2 vs 4	ns
	3 vs 4	0.028		3 vs 4	ns
IFN-γ^+ TNF-α^+ IL-2^-	1 vs 2	0.007	IFN-γ^- IL-4^- IL-13^+	1 vs 2	ns
	1 vs 3	ns		1 vs 3	0.016
	1 vs 4	0.007		1 vs 4	0.009
	2 vs 3	ns		2 vs 3	0.028
	2 vs 4	0.009		2 vs 4	0.009
	3 vs 4	0.009		3 vs 4	0.009
IFN-γ^+ TNF-α^- IL-2^+	1 vs 2	ns	IFN-γ^- IL-4^+ IL-13^+	1 vs 2	ns
	1 vs 3	ns		1 vs 3	ns
	1 vs 4	0.009		1 vs 4	ns
	2 vs 3	ns		2 vs 3	ns
	2 vs 4	0.009		2 vs 4	ns
	3 vs 4	0.009		3 vs 4	ns

$^{\Omega}$Groups: 1 = Placebo, 2 = Ag only, 3 = Ag + Alhydrogel and 4 = Ag + MF59C.1

$^{\Psi}$ *P*-values were calculated as described in Supplementary table 2.

Supplementary table 5. *P*-values for the $CD3^+CD8^+$ T cell data in Figure 3d

Population	Groups$^{\Omega}$ compared	$^{\Psi}$ *P*-value	Population	Groups compared	*P*-value
IFN-γ^+ TNF-α^- IL-2^-	1 vs 2	ns	IFN-γ^- TNF-α^+ IL-2^+	1 vs 2	ns
	1 vs 3	ns		1 vs 3	0.047
	1 vs 4	0.009		1 vs 4	ns
	2 vs 3	ns		2 vs 3	0.026
	2 vs 4	0.009		2 vs 4	0.009
	3 vs 4	0.009		3 vs 4	ns
IFN-γ^- TNF-α^+ IL-2^-	1 vs 2	ns	IFN-γ^+ TNF-α^+ IL-2^+	1 vs 2	ns
	1 vs 3	ns		1 vs 3	<0.001
	1 vs 4	0.028		1 vs 4	<0.0001
	2 vs 3	ns		2 vs 3	ns
	2 vs 4	0.047		2 vs 4	ns
	3 vs 4	ns		3 vs 4	ns
IFN-γ^- TNF-α^- IL-2^+	1 vs 2	ns	IFN-γ^- IL-4^+ IL-13^-	1 vs 2	ns
	1 vs 3	ns		1 vs 3	ns
	1 vs 4	ns		1 vs 4	0.047
	2 vs 3	ns		2 vs 3	ns
	2 vs 4	0.016		2 vs 4	ns
	3 vs 4	0.047		3 vs 4	ns
IFN-γ^+ TNF-α^+ IL-2^-	1 vs 2	ns	IFN-γ^- IL-4^- IL-13^+	1 vs 2	ns
	1 vs 3	ns		1 vs 3	ns
	1 vs 4	0.037		1 vs 4	0.009
	2 vs 3	ns		2 vs 3	ns
	2 vs 4	0.005		2 vs 4	0.016
	3 vs 4	<0.0001		3 vs 4	0.009
IFN-γ^+ TNF-α^- IL-2^+	1 vs 2	ns	IFN-γ^- IL-4^+ IL-13^+	1 vs 2	ns
	1 vs 3	ns		1 vs 3	ns
	1 vs 4	0.034		1 vs 4	ns
	2 vs 3	ns		2 vs 3	ns
	2 vs 4	0.034		2 vs 4	ns
	3 vs 4	ns		3 vs 4	ns

$^{\Omega}$Groups: 1 = Placebo, 2 = Ag only, 3 = Ag + Alhydrogel and 4 = Ag + MF59C.1

$^{\Psi}$ *P*-values were calculated as described in Supplementary table 2.

Supplementary table 6. Histopathology findings from hamster two dose study.

	Peribronchial / Perivascular cuffing		**Alveolar Oedema**		**Alveolar Hemorrhage**	
	Day 4	Day 8	Day 4	Day 8	Day 4	Day 8
Placebo	5/5	4/5	0/5	4/5	0/5	2/5
Inactivated virus + Alhydrogel	3/5	3/5	2/5	0/5	3/5	0/5
Sclamp + MF59C.1	1/5	1/5	1/5	0/5	1/5	0/5
Infection and Recovery	1/5	0/5	0/5	0/5	1/5	0/5

Supplementary Data for Manuscript Entitled
Preclinical development of a Molecular Clamp Stabilised Subunit Vaccine for SARS-CoV-2

SUPPLIMENTERY REFERENCES

1. McLellan JS, Chen M, Leung S*, et al.* Structure of RSV fusion glycoprotein trimer bound to a prefusion-specific neutralizing antibody. *Science* 2013; **340**: 1113-1117.
2. Wen X, Mousa JJ, Bates JT, Lamb RA, Crowe JE, Jr., Jardetzky TS. Structural basis for antibody cross-neutralization of respiratory syncytial virus and human metapneumovirus. *Nat Microbiol* 2017; **2**: 16272.
3. Mousa JJ, Kose N, Matta P, Gilchuk P, Crowe JE, Jr. A novel pre-fusion conformation-specific neutralizing epitope on the respiratory syncytial virus fusion protein. *Nat Microbiol* 2017; **2**: 16271.
4. Friesen RH, Lee PS, Stoop EJ*, et al.* A common solution to group 2 influenza virus neutralization. *Proc Natl Acad Sci U S A* 2014; **111**: 445-450.
5. Corti D, Voss J, Gamblin SJ*, et al.* A neutralizing antibody selected from plasma cells that binds to group 1 and group 2 influenza A hemagglutinins. *Science* 2011; **333**: 850-856.